Eleventh International Conference on CFD in the Minerals and Process Industries
CSIRO, Melbourne, Australia
7-9 December 2015

NUMERICAL SIMULATION OF SLAG FOAMING IN OXYGEN STEELMAKING

Anuththara K. HEWAGE, Jamal NASER*, Geoffrey BROOKS

Faculty of Science, Engineering and Technology, Swinburne University of Technology, Hawthorn, Victoria 3122, AUSTRALIA
*Corresponding author, E-mail address: jnaser@swin.edu.au

ABSTRACT

The extent of refining in the oxygen steelmaking converter depends on the chemical and physical properties of the bath. The high speed oxygen jet injected on to the bath in this process oxidises the elements forming the slag, and the evolving chemical composition and the physical properties of this slag causes it to foam. The phenomenon of slag foaming can become disastrous and the need of a dynamic model for understanding slag foaming has been emphasized in the literature. Therefore in the present work, the numerical model developed by Sattar (2013) for predicting the foam height in oxygen steelmaking was further improved to incorporate the slag components in the liquid phase, simultaneously with the kinetics of refining reactions in the bath.

The new liquid phase consists of the oxides formed from iron, silicon, manganese and phosphorus together with the elements. Continuous mass and momentum interactions occur between each phase in the model. The foam phase is then formed by the interaction between the liquid (i.e. liquid metal and oxides) and gas phases, in contrast to the foam generated by pure liquid in the original model by Sattar et al. (2013a). Formation of slag foam in steelmaking and its lifetime are known to depend on many parameters including the physical properties and the chemical composition of the slag (i.e. density, viscosity and effective surface tension). Therefore the evolution of these physical properties' and the chemical composition was taken into account through separate user subroutines in the model.

The results obtained from the model for the slag foam height and the chemical composition of the molten metal bath over time were compared with the published pilot plant data in Millman et al. (2011) and were in good agreement with the observed data.

NOMENCLATURE

BOS:	*Basic Oxygen Steelmaking*
BOF:	*Basic Oxygen Furnace*
IMPHOS:	*IMproving PHOSphorus refining*

INTRODUCTION

Oxygen steelmaking is one of the major processes for producing steel from pig iron globally. In this process, a high speed oxygen jet is injected onto the bath and the impurity elements in the bath are oxidised and removed from the molten metal bath to produce steel. These highly exothermic oxidising reactions produce oxides of the elements in the bath, simultaneously raising the temperature of the bath, further increasing the reaction rates. The oxides produced (e.g. SiO_2, CO, P_2O_5 and MnO) and the added fluxes form a slag, of which the physical properties change over time due to the constantly changing chemical composition. Since this slag has a high viscosity and low surface tension compared to the liquid metal, the gasses produced in the reactions are trapped in the slag layer producing slag foam.

Slag foaming can result in significant process disturbances when formed in excessive amounts. The high rates of gas and slag generation give rise to extensive slag foaming and can cause an event commonly known as slopping. In order to control the slag foaming, the traditional method was to observe the process and physically control the process variables like the lance height, which depends on the capability and the experience of the operator. Therefore researchers have been involved in modelling the slag foaming in oxygen steelmaking, so that the production process can be better controlled and optimized with fewer interruptions to the continuous production of steel.

Slag foaming is well established to be dependent on the physical properties of the slag and the rate and quantity of gas generation. Among the several studies available in the literature on understanding the slag foaming, the experimental work done by Fruehan and the co-workers (Ito and Fruehan (1989), Jiang and Fruehan, 1991, Jung and Fruehan, 2000, Zhang and Fruehan, 1995) showed that the foaming index (i.e. foaming capacity of the slag) mainly increases with the increasing slag viscosity, and decreases with the increasing slag density and surface tension. These factors were further investigated by Hayes et al (Ghag et al., 1998a, Ghag et al., 1998b, Ghag et al., 1998c). On the other hand, Gou et al. (1996) argued that at those higher gas generation rates, the liquid bath is "held up" and this behaviour is different from the classic foaming phenomena. In this circumstance the "foaming" mainly depends on the void fraction and is less dependent on the physical properties of slag.

However, most of these studies are limited to laboratory experiments and have limitations when used to analyse the real oxygen steelmaking process. Therefore there is a need for an improved foaming model to replicate the actual slag foaming process. Slag foaming, as explained earlier, is evolving over time in the BOF. Hence the models also have to be dynamic in order to capture this dynamic phenomenon and predict the process parameters over time. A few researchers have addressed this issue including Sattar (2013) by developing a numerical model to predict the foam height over time in oxygen steelmaking.

The model developed by Sattar et al. (2013b) was capable of predicting the results obtained by Jiang and Fruehan (1991) on slag foam height evolution over time in an experiment with injecting Ar gas into a crucible, containing steelmaking slag. This model was then extended by the same authors to predict the foam height in the actual steelmaking process. The published data by (Millman et al., 2011) from trials carried out in a BOS pilot plant were used to extract information on the model geometry and details of the heats.

Further, in the foaming model proposed by Sattar and the co-workers (Sattar et al., 2013a, Sattar et al., 2013b, Sattar et al., 2013c), the foam was generated when the gas volume fraction is more than or equal to 75% in a cell and then the gas and liquid in the cell were transferred into foam. The foam then suddenly collapses due to the absence of any proper surface active compound and returns to liquid and gas. In the foam phase 10 bubble classes were considered and the density and the viscosity of the foam phase were calculated using the bulk properties of the liquid and the gas. Further foam bubble coalescence was considered based on film rupture in the foam phase. Although this model was predicting the foam height with good agreement compared to the plant data (Figure 1), the model had several drawbacks when applied to the real slag foaming phenomena in oxygen steelmaking.

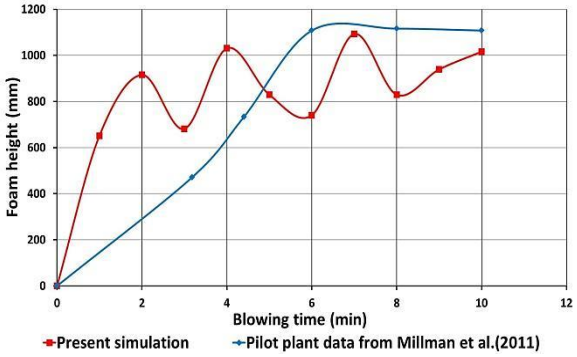

Figure 1: Slag foam height vs. time (Sattar, 2013)

In order to analyse the actual steelmaking process, the model has to be further improved in terms of the chemical composition's and physical properties' evolution over time. The limitations in the model by Sattar (2013) include the inadequate number of chemical reactions incorporated, modelling with only one liquid phase (i.e. only the liquid metal) and not addressing the effect of physical properties of slag on foaming and foam drainage, when compared to the actual steelmaking process.

In the model, the liquid phase consists of liquid components and slag components. Although, in actual steelmaking process, liquid metal and the slag are considered two different phases, in the present work, both the slag and the liquid metal are considered to be one phase with the name 'liquid'. The model identifies the difference between the slag and metal by the density difference. The performance of the foaming criteria which was used in this model (Sattar, 2013) was initially developed and validated for liquid foams and has to be improved to approximate the slag foaming phenomena.

Therefore in the present work, the previously explained model was extended to include the other major chemical reactions and an improved foaming model. Then the results for foam height and the kinetics of the elements carbon, silicon, manganese and phosphorus were analysed and compared with the data published by (Millman et al., 2011).

MODEL DESCRIPTION

The model geometry used in the present simulation is shown in Figure 2 and it is similar to that used by Sattar (2013). It is a schematic diagram of a 6 t MEFOS pilot plant BOS converter used for the IMPHOS research work (Millman et al., 2011). A 3D thin slice of that geometry was used in the present simulation as shown in Figure 3. The surface mesh of the model was developed in CAD software Rhinoceros 3.0 and imported in CFD simulation software AVL FIRE 2009.2 to generate volume mesh of the model. The height and the diameter of the model were 2.905m and 1.340m respectively while the height of the initial molten metal height was 0.660m.

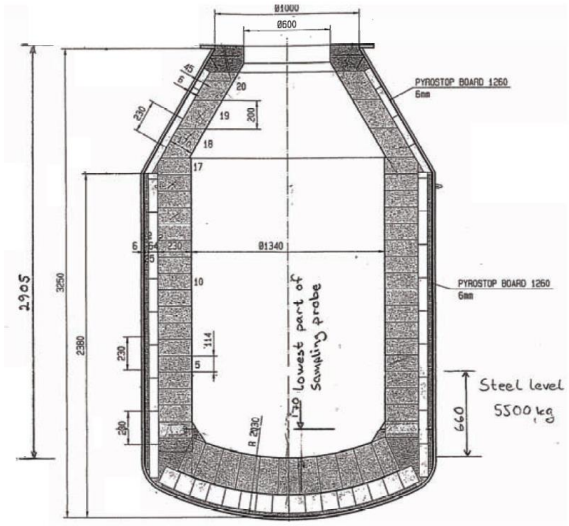

Figure 2: Schematic diagram of the 6 tonne BOS converter (Millman et al., 2011).

The simulation was run on an Intel(R) Xenon(R) CPU E5-1620 0 machine, where the RAM and the speed of the processor are 16GB and 3.60GHz respectively. Transient kinetics results were calculated for a time step of 0.001s for 8 minutes in real time. The software (AVL FIRE 2009.2) is based on the finite volume approach and the multiphase flow simulation was carried out using an Eulerian-Eulerian approach. All the phases interact with each other in terms of mass, momentum and energy. The following conditions were used in the simulation (Kalyani et al., 2014).

- Liquid phase is incompressible.
- Unsteady state multiphase solution is used for momentum and continuity.
- A standard k-ε model is used for turbulence.
- First order upwind differencing scheme is used for momentum and turbulence.
- Second order central differencing scheme is used for continuity equation.

User subroutines were written using the FORTRAN programming language to incorporate the chemical reactions and physical properties (density and viscosity) in the main numerical program.

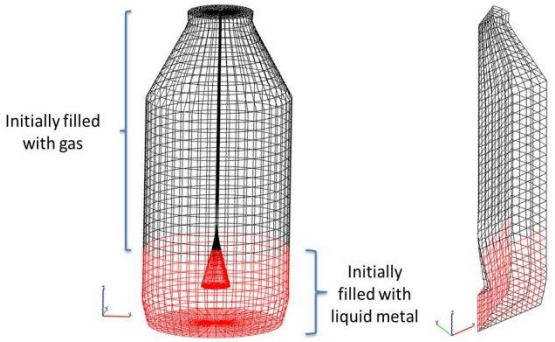

Figure 3: 3D model of the Oxygen Steelmaking converter and the thin slice of the model used for the simulation.

Oxygen was continuously injected on to the liquid metal through an extended lance tip (Sattar, 2013) located in the middle of the converter. The temperature of the input oxygen stream was same as that of the liquid bath which was assumed to be 1650K and the liquid bath was steady in the converter. Normal velocity boundary conditions were applied for all the three phases at the inlet. At the outlet, which was on the top surface of the converter, the static pressure boundary condition was applied. The walls of the model were considered as non-slip and were at the same fixed temperature as the liquid bath. The properties of the foam were calculated according to the relationships used by Sattar et al. (2013b).

INTRODUCED KINETICS MODEL

The incorporation of the major chemical reactions was the first stage of the simulation. In oxygen steelmaking the injected oxygen oxidise the impure elements: silicon, manganese, phosphorus and carbon. CO and CO_2 are produced in the decarburisation reaction and the products of other oxidising reactions (i.e. FeO, SiO_2, MnO and P_2O_5) form the slag. Therefore the chemical reactions included in the model, consist of the major oxidising reactions, as shown below and refining reactions between slag and liquid components in the liquid phase.

$$[C] + [O] = CO_g$$
$$Fe + [O] = (FeO)$$
$$[Si] + 2[O] = (SiO_2)$$
$$[Mn] + [O] = (MnO)$$
$$2[P] + 5[O] = (P_2O_5)$$
$$CO_{(g)} + (1/2)O_{2(g)} = CO_{2(g)}$$

Although the kinetics of steelmaking are known to be more complex, a simple first order kinetics relationship was assumed for incorporating the above mentioned chemical reactions in the model. It is established that the reactions in steelmaking bath are often governed by the diffusion of the reactants to the slag-metal interface as they occur at high temperatures in the converter. Therefore Fick's law of diffusion was used in the present work as given by equation 1 to determine the quantity of the reactants available reacting in each cell.

$$\frac{dC}{dt} = kA\frac{\rho_m}{WM}(C_b - C_{eq}) \quad (1)$$

Where:
C: Concentration of the elements (wt %)
k: Mass transfer coefficient (m/s)
A: Interfacial area (m^2)
ρ_m: Density of the metal (kg/m^3)
WM: Weight of the metal (kg)
C_b: Bulk concentration of the elements in the metal (wt %)
C_{eq}: Equilibrium concentration of the elements in the metal (wt %)

The value of the constant (kA), in equation 1 was calculated using the method proposed by Deo and Boom (106-145, 1993). The input data were extracted from the IMPHOS report (Millman et al., 2011) and the details of the calculation procedures is published in a separate paper (Hewage et al., 2015).

The above relationship (equation 1) was then re-arranged into the following relationship to be used in the subroutines for the model.

$$\frac{dC}{dt} = K(m_{f_{b,i}} - m_{f_{eq,i}})\alpha_l\rho_l v_c \quad (2)$$

Where,
C: Mass fraction of the element in the cell
K: Constant (k × A)
$m_{f_{b,i}}$: Bulk mass fraction of the element in the cell.
$m_{f_{eq,i}}$: Equilibrium mass fraction of the element.
α_l: Liquid volume fraction.
ρ_l: Density of liquid. (kg/m^3)
v_c: Volume of the cell. (m^3)

(2) ➡ $$\frac{dC}{dt} = K(m_{f_{b,i}} - m_{f_{eq,i}}) \quad (3)$$

The quantity of the reactants reacted was limited by the oxygen availability.

$$\frac{dO_2}{dt} = O_{2_{available}} r_f \quad (4)$$

The eddy break-up equation was incorporated in order to include the effect of turbulence in the converter (Bai and Fuchs, 1994).

$$R_{f,MH} = A\rho\min(m_f - \frac{m_{O_2}}{r_f})\frac{\epsilon}{k} \quad (5)$$

(3), (4) ➡ (5) $$\frac{dC}{dt} = A\min(dC, dO_2)\frac{\epsilon}{k}\alpha_l\rho_l v_c \quad (6)$$

Where,
A: Constant
dC: Mass of reacted element. (kg)
dO_2: Mass of reacted oxygen. (kg)
m_f: Mass fraction of the element in the cell.
m_{O_2}: Mass fraction of oxygen in the cell.
ϵ: Multiphase dissipation rate. (m^2/s^3)
k: Multiphase turbulence kinetic energy. (m^2/s^2)
r_f: stoichiometry constant of the reaction.

INTRODUCED CHANGES TO THE SLAG FOAM SIMULATION

In oxygen steelmaking, foam is formed by trapping gas bubbles in the slag layer due to the increased viscosity and surface tension of the slag compared to the liquid metal. However, slag foam can be studied by approximating it to well-drained foam of soap solution (Nexhip et al., 1998), where the structure of the foam is similar to that of foam generated from a mixture of gas and liquid as assumed by the Sattar et al. (2013a). In the slag foam, the foam is generated by slag which mainly consists of oxides and added fluxes during the steelmaking process. Further, it is established that the slag foam consists mainly of spherical small bubbles with diameters less than 1mm, produced by CO generated from the decarburization reaction (Zhang and Fruehan, 1995, Kitamura and Okohira, 1992). Therefore the slag foam during the blow can be considered as consisting of a liquid fraction from 0.05 to 0.12 (Koehler, 2012).

The components in the slag such as the P_2O_5, tend to reduce the surface tension of the slag and components such as SiO_2 tend to increase the viscosity. Therefore the physical properties such as viscosity and the surface tension of the liquid metal bath constantly vary due to the addition of those compounds (i.e. SiO_2, CaO, P_2O_5 and FeO). With the increase of viscosity and the decrease in the surface tension, the slag foam drainage is retarded with time as shown in figure 4, where the critical thickness before the rupture of the foam bubble film reached 0.1 to 0.4 μm in the experimental studies carried out by Nexhip et al. (1998).

Therefore in the present study, the foam formation criteria developed by Sattar et al. (2013a) was further improved by combining minimum requirement of 0.05 of liquid mass fraction in the cell. This was according to the previous explained requirement of minimum 5% liquid mass fraction for a foam with spherical bubbles. Constant drainage of the foam was calculated according to the equation 7 and the drainage was allowed until the critical liquid volume fraction was reached in foam phase, which was assumed to be 0.01. When the foam reached this critical liquid fraction in foam, the foam phase collapses and the masses of liquid and gas, that were in the foam, were returned to liquid and gas phases according to the same criteria used by Sattar et al. (2013a).

$$q_{PB} = \frac{1}{5} \mathrm{NR} n_p a_p u \qquad (7)$$

Where:

q_{PB}: Liquid volume flux through the plateau border channels (m^3/s)
NR: Number of foam bubbles of radius R intersecting the plane (Sattar et al., 2013b)
n_p: Number of plateau border channels
a_p: Plateau border area (m^2)
u: Drainage velocity (m/s)

The geometry of the foam bubbles was considered to be the same as Sattar et al. (2013a) and the drainage velocity was calculated by the bulk properties of the liquid metal. The deceleration of the drainage due to increasing viscosity and decreasing density are not considered in this model.

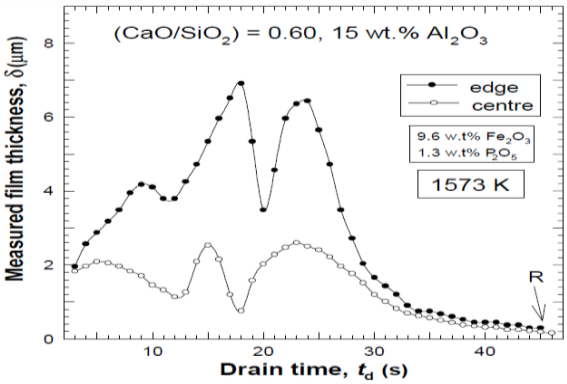

Figure 4: Drainage of film over time (Nexhip et al., 1998)

RESULTS

The results obtained from the model for the removal of impurity elements (carbon, silicon, manganese and phosphorus) are shown in the figure 5 to 8 and the foam height results are shown in figure 9, (In this stage of the model, the foam simulation does not include the foam drainage). The observed results obtained from the IMPHOS report are also plotted for the purpose of comparison together with the model predictions.

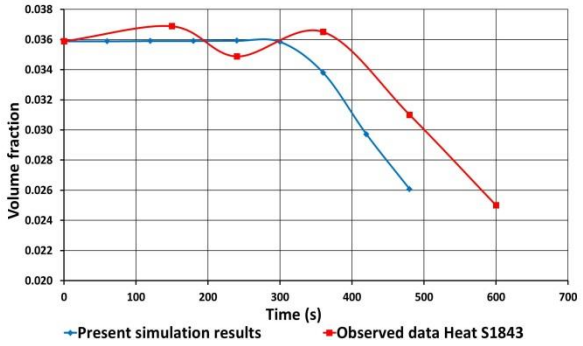

Figure 5: Carbon removal behaviour.

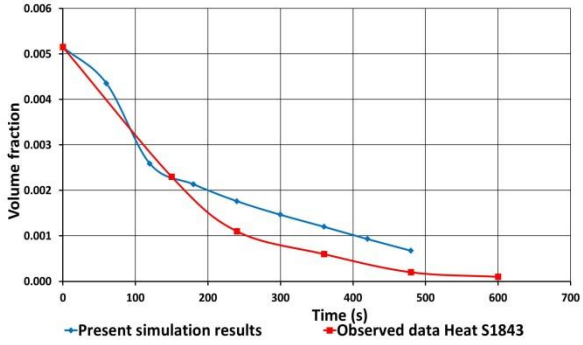

Figure 6: Silicon removal behaviour.

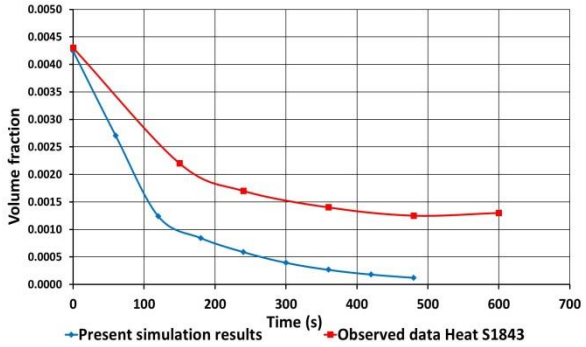

Figure 7: Manganese removal behaviour.

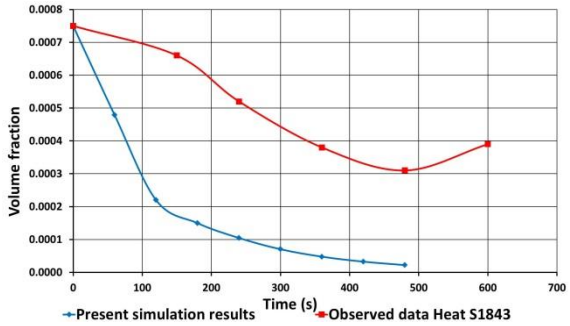

Figure 8: Phosphorus removal behaviour.

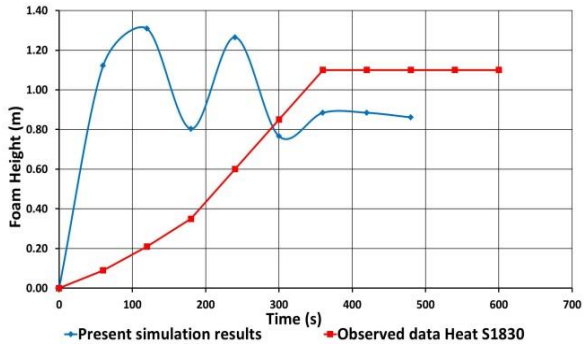

Figure 9: Foam height evolution over time.

According to the figures 5 and 6, the model predictions for the removal of carbon and silicon are in good agreement with the observed data. Since the decarburization reaction starts after about 3 minutes in the actual process, the reaction was intentionally stopped for 3 minutes. Although the reaction rate is over-predicted, the decarburization closely follows the actual carbon removal behavior. The desiliconization reaction rate is also predicted by the model with a good degree of fit to the observed silicon removal behaviour.

The model predictions on the removal of manganese and phosphorus are over-predicted as shown in figures 7 and 8. Demanganization and dephosphorization reactions are well-known to depend on the chemical composition of the slag and liquid metal as well as on the bath temperature. In the present simulation the evolution of the slag chemical composition was not incorporated in the model and therefore, the removal behaviour of manganese and phosphorus was not well-predicted by the model.

The main aim of the present simulation was to obtain a better foam height prediction. As shown in figure 9, the model foam height prediction is over-predicted towards the start of the blow with a considerable variation and stabilises at a lower foam height after about 6 minutes compared to the observed data. Although it is mentioned in the IMPHOS report that slopping was observed after 10 minutes, the model at this stage is not predicting the probability of slopping. But during the 10minutes time period model predicts the average maximum foam height with a good degree of fit.

Figure 10 shows the results of foam height obtained from the model when the proposed improvements to the foaming model were implemented. The simulation was run and transient kinetics results were calculated for a time step of 0.001 seconds for 5 minutes in real time.

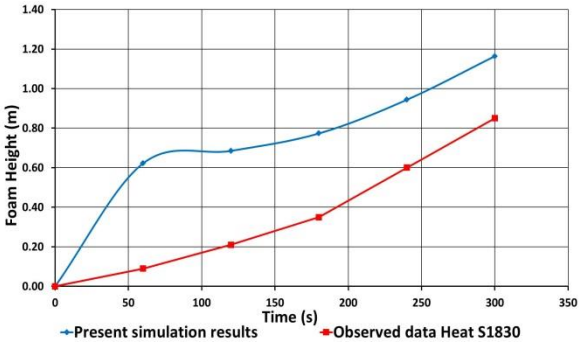

Figure 10: Foam height evolution over time with improved slag foaming criteria.

The foam height prediction from the model with the improved foam formation criteria has improved when compared to the previous results without the improvements. In the foam height prediction in figure 9, a variation of foam height prediction can be seen within the first 5 minutes, but with the improved foam model (Figure 10), that instability of foam height is stabilised to a certain extent. Also the foam height prediction has become more accurate in the first 5 minutes of the blow. However more work is being done on the foam drainage and the kinetics to improve the model further.

CONCLUSION

The importance of a slag foaming model for oxygen steelmaking is emphasized in the literature, because the extensive slag foaming in a steelmaking converter can cause damage to the property and the shop floor people as well as can cause interruptions to the continuous production process. Although several studies on understanding and modelling slag foaming are available, most of them are laboratory scale studies and have limitations when applied to plant scale steel production, specifically the dynamic nature of the real steelmaking process is not captured and modelled.

Therefore in the present study, the foaming model developed by Sattar (2013) was extended to incorporate the kinetics model with all major chemical reactions and the improved foaming criteria developed by the authors. The simulation results obtained for the removal behaviour of carbon and silicon were in good agreement with the

observed data while those for the removal of manganese and phosphorus were over-predicted. This over-prediction may be due to the absence of a proper slag generation model.

The foam height prediction of the model was over-predicted at the start of the process, but reached the observed data towards the end of about 10 minutes. The foam height exhibited a huge variation at the start and stabilises towards the end of 6 minutes slightly below the observed foam height data. The results of the model with the improved foaming phenomenon shows that the proposed alterations have improved the model predictions on the slag foam height, but further work is required on the foaming model.

Therefore future work involves improving the present model further by incorporating more accurate kinetics model with a separated slag phase, so that the chemical composition of the slag formed can be better predicted and thereby improve the prediction of demanganization and the dephosphorization. Also the changing physical properties due to changing chemical composition of the liquid phase with the added and produced slag components will be incorporated for improving the foaming model.

REFERENCES

BAI, X. S. & FUCHS, L. 1994. Modelling of Turbulent Reating Flows past a Bluff Body: Assessment of Accuracy and efficiency. *Computers Fluids,* 23**,** 507-521.

DEO, B. & BOOM, R. 106-145, 1993. *Fundamentals of steelmaking metallurgy,* New York, Prentice Hall international.

GHAG, S. S., HAYES, P. C. & LEE, H. G. 1998a. Model Development of Slag Foaming. *ISIJ International,* 38**,** 1208-1215.

GHAG, S. S., HAYES, P. C. & LEE, H. G. 1998b. Physical Model Studies on Slag Foaming. *ISIJ International,* 38**,** 1201-1207.

GHAG, S. S., HAYES, P. C. & LEE, H. G. 1998c. The Prediction of Gas ResidenceTimes in Foaming CaO-Si02-FeO Slags. *ISIJ International,* 38**,** 1216-1224.

GOU, H., IRONS, G. A. & LU, W. K. 1996. A Multiphase Fluid Mechanics Approach to Gas Holdup in Bath Smelting Processes. *Metallurgical and Materials Transactions B,* 27B**,** 195-201.

HEWAGE, A. K., ROUT, B. K., BROOKS, G. & NASER, J. 2015. Analysis of steelmaking kinetics from IMPHOS pilot plant data. *Ironmaking & Steelmaking***,** 1743281215Y.000.

ITO, K. & FRUEHAN, R. J. 1989. Study on the Foaming of CaO-SiO2-FeO Slags: Part I. Foaming Parameters and Experimental Results. *Metallurgical Transactions B,* 20B**,** 509-514.

JIANG, R. & FRUEHAN, R. J. 1991. Slag Foaming in Bath Smelting. *Metallurgical Transactions B,* 22B**,** 481-489.

JUNG, S.-M. & FRUEHAN, R. J. 2000. Foaming Characteristics of BOF Slags. *ISIJ International,* 40**,** 348-355.

KALYANI, K. H. A., NASER, J. & BROOKS, G. Preliminary Numerical Simulation of Chemically Reacting Gas and Liquid Phases in Oxygen Steelmaking. 19th Australasian Fluid Mechanics Conference, 2014 Melbourne, Australia.

KITAMURA, S. & OKOHIRA, K. 1992. Influence of Slag Composition and Temperature on Slag Foaming. *ISIJ International,* 32**,** 741-746.

KOEHLER, S. A. 2012. Foam Drainage. *In:* STEVENSON, P. (ed.) *Foam Engineering.* John Wiley & Sons, Ltd.

MILLMAN, M. S., KAPILASHRAMI, A., BRAMMING, M. & MALMBERG, D. 2011. Imphos: Improving Phosphorus Refining. Luxembourg: European Commission, Research Fund for Coal and Steel.

NEXHIP, C., SUN, S. & JAHANSHAHI, S. 1998. Studies on Bubble Films of Molten Slags. *Phil. Trans. R. Soc. Lond. A,* 356**,** 1003-1012.

SATTAR, M. A. 2013. *Numerical Simulation of Foaming in Metal Processing with Population Balance Modelling.* Doctor of Philosophy, Swinburne University of Technology.

SATTAR, M. A., NASER, J. & BROOKS, G. 2013a. Numerical Simulation of Creaming and Foam Formation in Aerated Liquid with Population Balance Modeling. *Chemical Engineering Science,* 94**,** 69-78.

SATTAR, M. A., NASER, J. & BROOKS, G. 2013b. Numerical Simulation of Slag Foaming in High Temperature Molten Metal with Population Balance Modeling. *Procedia Engineering,* 56**,** 421-428.

SATTAR, M. A., NASER, J. & BROOKS, G. 2013c. Numerical Simulation of Two-Phase Flow with Bubble Break-up and Coalescence Coupled with Population Balance Modeling. *Chemical Engineering and Processing: Process Intensification,* 70**,** 66-76.

ZHANG, Y. & FRUEHAN, R. J. 1995. Effect of Bubble Size and Chemical Reactions on Slag Foaming. *Metallurgical and Materials Transactions B,* 26B**,** 803-812.

